IEEE Access
Multidisciplinary | Rapid Review | Open Access Journal

Received 10 July 2023, accepted 27 July 2023, date of publication 2 August 2023, date of current version 9 August 2023.

Digital Object Identifier 10.1109/ACCESS.2023.3301173

RESEARCH ARTICLE

Survivable Network Slicing Using Shared Link Protection

NOURHAN REZK, MOHAMED SHEHATA, (Member, IEEE), SAFA M. GASSER, (Member, IEEE), AND MOHAMED S. EL-MAHALLAWY

Department of Electronics and Communications, Arab Academy for Science, Technology and Maritime Transport, Cairo 11799, Egypt

Corresponding author: Nourhan Rezk (N.Ahmed3069@student.aast.edu)

ABSTRACT In optical metro-aggregation networks, logical partitioning or network slicing can enforce the high reliability required by advanced services. This can be achieved by enabling flexible resource management. Virtual network functions composing a slice can be deployed over physical nodes using different strategies. In reliable network slicing, a virtual network request involves allocating link-disjoint primary and backup resources to protect against single link failure. In this paper, we present a reliable virtual network embedding algorithm over elastic optical networks considering shared link protection (SLP). This is to reduce the required backup resources. We propose a heuristic SLP mapping algorithm that enables the multiplexing of S primary links to share the same backup resource on a given backup link, offering improved resource utilization. We extend our proposed SLP algorithm to be represented by *mapping matrices*. These matrices define the mapping of S sharing links on a physical link as well as the required sharing capacity. SLP is shown to perform remarkably better than dedicated link protection and allows efficient wavelength channel utilization by reducing the backup resources needed for protection by up to 37%.

INDEX TERMS Dedicated link protection, network slicing, reliability, shared link protection, wavelength division multiplexing (WDM) metro-aggregation network.

I. INTRODUCTION

The necessity to provide high-quality network services with high user demand has accelerated the development of the next-generation 5G network architecture. In 5G New Radio (NR), various mobile services require bandwidth, compute, latency, and reliability needs. These new services are classified into three main categories; enhanced Mobile Broadband (eMBB), ultra-Reliable Low-Latency Communication (uRLLC), and massive Machine Type Communication (mMTC) [1]. Network virtualization has recently become a subject of interest for many researches by providing multiple tenants/services to share the same physical substrate network [2]. These services are supported by elastic optical network (EON), which is a crucial technology for the next generation network paradigm due to its potential to improve network resource efficiency and flexibility. A major challenge in EON is the so-called virtual network embedding (VNE), which can be defined as mapping a virtual network (VN) efficiently over a substrate physical network in order to meet the expected network traffic demand [3], [4]. Further, to achieve flexible resource management, network function virtualization (NFV) [5] and software-defined networking (SDN) [6] are introduced. The authors of [7] combined the properties of NFV and SDN to fully exploit the advantages of flexible and convenient network functions. In this context, NFV and SDN allow scaling up/down services to meet user fluctuating demand. In addition, they can reduce capital expenditure (CAPEX) and operational expenditure (OPEX) through low cost agile network infrastructures [8].

Recently, network slicing has been introduced to accommodate various and stringent service requirements [9]. Network slicing allows multiplexing of virtualized multiple logical independent slices to share the same physical network. To achieve flexible resource management, network slicing can be applied to optical metro-aggregation networks. Each network slice is represented by radio access network (RAN) functions that can be tailored according to

The associate editor coordinating the review of this manuscript and approving it for publication was Tianhua Xu.

service requirements. RAN functional split problem is considered to have a pivotal role for both the research and the industry. Flexible functional split allows mobile network operators (MNOs) to gather the benefits of different split options according to their needs. Due to scalability limitations in 4G RAN architecture, flexible 5G functional split has been extensively studied by distributing RAN functions on a 3-layer architecture featuring a radio unit (RU), a distributed unit (DU), and a central unit (CU) [10]. Flexible RAN virtualization and functional split options are detailed in [11] and [12].

Due to the simultaneous coexistence of multiple slices sharing the same physical infrastructure, network slicing must ensure a certain level of isolation, which is determined by the slice's specific requirements. In consequence, any security threat can affect only a certain slice without affecting other slices [10], [13]. The authors of [14] categorize isolation to virtual network functions (VNFs) isolation and network isolation, and show how different levels of isolation can impact resource usage considering reliable slicing. It is important to note that lightpaths in traditional WDM networks cannot overlap and have fixed-grid, rigid bandwidths [15].

In network slicing, one of the main challenges is ensuring a resilient and survivable network to prevent unplanned downtime and outages. Network survivability is defined as how to maintain the service even in the presence of network failures/attacks (e.g. fiber cable cuts, environmental hazards or human errors) [16], [17]. To provide slice protection, it is necessary to consider the entity to be protected (e.g. links, nodes, sub-paths, end-to-end), the provisioning method of backup resources (dedicated protection, shared protection), and the protection layer (physical, such as WDM, or logical, such as IP) [14]. Traditionally, to provide reliability against link failures, which is the focus of our paper, a survivable network must involve the establishment of a primary link and a backup (i.e. recovery) link. The methods of ensuring survivability can be divided into two categories: protection and restoration. Protection schemes typically involve pre-establishing backup resources prior to failure, resulting in high resource utilization but faster recovery time. However, in restoration schemes, backup resources are established after failure occurrence [18], hence, it has higher recovery time than protection schemes and better resource utilization [19]. In this paper we will study protection schemes, which are less resource-efficient but provide faster recovery time. Network survivability techniques can be further classified into path or link-based, and dedicated or shared backup protection.

In path-based schemes, an alternative disjoint route is provided between source and destination nodes (i.e. both the primary path and the backup path are node disjoint). Thus, it has the benefit of service recovery in case of either node or link failures, however, requires mapping of the VNFs over different nodes of the backup path. Link-based schemes, on the other hand, only provide an alternative disjoint route between the end nodes of the failed link. A link-based scheme has lower resource efficiency than a path-based scheme in terms of link usage as it utilizes more recovery links. With regard to availability, path protection provides less availability than link protection [20]. This is due to the need to find available backup links between source and destination nodes. In link protection, however, only backup links between nodes of failed links need to be found.

Dedicated backup protection schemes are classified into 1+1 protection and 1:1 protection, while shared backup protection schemes are classified into 1:N protection and M:N protection. In 1+1 protection, traffic is replicated and transmitted on both the primary and the backup path/link, whereas in 1:1 protection, traffic is only transmitted on the primary path/link during normal operation and switches to the backup path/link only if the primary path/link fails. Although dedicated backup protection techniques provide instantaneous recovery from failures, they consume a significant number of network resources. To reduce network resources usage, shared backup protection techniques are provided. In 1:N protection, one protection unit is reserved for N sharing units, while in M:N protection ($M \leq N$), M protection units are reserved for N sharing units. Shared backup protection techniques are more resource efficient than dedicated backup protection techniques, however, they have more design complexity as they involve multiplexing of multiple links to share the same backup resources [21]. In addition, failure detection is still needed in shared backup protection techniques, which may slow down recovery. In order to reduce network resource usage, while still providing instantaneous recovery, network coding protection is introduced in literature to achieve both advantage of dedicated protection and shared one [22]. A common circuit is designed to transmit signals from N connections such that, in the event of a failure, the end nodes of the connection affected by the failure will be able to recover the lost signals. Network coding is used to combine signals from multiple connections and transmit them over the backup circuit. In this manner, survivability is ensured without explicit failure detection, and no rerouting is necessary. The authors in [23] referred to this technique as 1+N protection.

A. PAPER CONTRIBUTION

To the best of our knowledge, existing works on link protection have only considered reliable slicing with dedicated link protection (DLP). In this paper, we propose a new reliable slicing technique for VNE problems considering shared link protection (SLP). The main goal of the proposed solution is to achieve efficient wavelength utilization by minimizing the backup resources needed for protection. The main contributions of the paper are summarized as follows:

- We formulate the problem of SLP reliable slicing with optimization objective subject to node and link constraints.
- We present a node mapping algorithm to perform RAN function placement with two different deployment

strategies, namely VNE and service function chaining (SFC).
- We introduce a link mapping algorithm to perform routing and wavelength assignment of primary and backup links for different network isolation models.
- We devise a new heuristic SLP mapping algorithm that enables the multiplexing of S primary links to share the same backup resource on a given backup link, offering improved resource utilization.
- Through a simulation study, we evaluate the performance of the proposed SLP solution compared to DLP in terms of wavelength channel utilization.

B. PAPER ORGANIZATION

The rest of this paper is organized as follows. In section II, we review related work. In section III, we discuss the system model and network architecture, problem formulation, slice request requirements, and a reliable slicing model with SLP. In section IV, we describe the proposed heuristic algorithm for node mapping, SLP mapping and link mapping. In section V, we perform numerical validation by comparing the proposed SLP to the conventional DLP model. The work is concluded in section VI.

II. RELATED WORKS

Many research papers address the reliability and survivability of communication networks. It is widely known that dedicated protection schemes utilize a large amount of backup resources, but guarantee rapid service recovery. The authors of [14] introduced a reliable slicing technique considering DLP at lightpath layer with different VNF and network isolation levels. An integer linear programming (ILP) model has also been formulated for routing, placement, and protection constraints.

Shared path protection (SPP) schemes have been proposed in the literature to overcome a single-link failure and also to gain efficient use of resources compared to dedicated path protection (DPP) [24]. However, SPP cannot assure service recovery in case of multi-link failures (i.e. when both primary and backup paths fail simultaneously). The work in [25] proposes a dynamic load balancing shared-path protection (DLBSPP) algorithm aiming to retrieve service in case of multi-link failures. Results show that DLBSPP achieves lower blocking probability, better spectrum utilization ratio and higher failure restoration ratio compared to conventional SPP algorithm. Similarly, the works in [26] and [27] have proposed multi-link failure strategies considering load balancing techniques, namely enhanced shared-path protection (ESPP) and self-organizing shared-path protection (SSPP). In [28], a survivable VNE over EON has been proposed considering shared path protection. An ILP model and a greedy-based approach have been formulated to minimize the VN requests rejection ratio. Results show 15% rejection ratio reduction using SPP compared to conventional DPP.

In [29], the authors investigated the problem of multi-access edge computing (MEC) location enhanced with protection schemes. In order to minimize the number of deployed MECs, the number of hosted slices and the service response time, a multi-objective genetic algorithm was presented. The authors extended the MEC location problem with 1:1 (i.e. dedicated) and 1:N (i.e. shared) path protection schemes. The authors of [30] addressed the problem of dynamic slice allocation considering both DPP and SPP schemes to ensure reliability against single node or link failure. A reconfiguration algorithm has also been proposed in order to adapt to changes in resource availability due to network changes as a result of slice activation and expiration. Results show that SPP has better performance than DPP for dynamic network management in terms of slice blocking probability and average bandwidth requirement per slice. Differentiated slice protection schemes in relation to service needs are studied in [31]. In more detail, to ensure high availability and fast recovery in case of failure, the authors assumed DPP for URLLC services, whereas SPP for the eMBB services in order to save resources for this highly demanding service class. An Optimization model is also introduced to minimize the number of active nodes and links and to guarantee service requirements. Path-based protection schemes significantly reduce resource consumption, however, it has lower resource availability compared to link-based schemes [20].

Recovery speed and redundant resources are the two key factors in determining dedicated or shared link protection. A number of studies have considered network coding and partial protection as a way to achieve a blend of dedicated and shared protection. Network coding involves encoding different signals under favorable conditions, and transmitting these encoded signals instead of sending individual signals. This reduces the network traffic load. Using partial protection strategies, services can tolerate a certain amount of degradation in failure events, which enables better spectrum utilization by reducing the protection traffic in the network. The emerging increase in traffic demand necessitates an innovative approach to better utilize the fiber capacity in optical transport networks. To reduce the effective traffic load for optical transport networks using optical-processing-enabled architectures, the authors in [32] propose a combined solution utilizing photonic network coding and partial protection techniques. In [22], the authors proposed dedicated protection schemes supported by network coding to improve network performance over conventional 1+1 routing. They formulate the problem as an ILP model to maximize network throughput under capacity constrained conditions. In [23], the authors proposed a network coding based protection scheme to protect against single and multiple link failures.This strategy involves receiving two copies of the same data unit, one on the working circuit and a second copy that can be extracted from linear combinations of data units transmitted on a shared protection path. As a result, data units are immediately recovered upon failure of a circuit. In [33], a new quality-of-service aware protection framework for the design of elastic optical networks with the capability of distance-adaptive and

reconfigurable modulation format assignment is provided. A QoS-aware traffic classification system with premium and best-effort types has been proposed. The authors were able to achieve greater spectrum efficiency by reconfiguring transmission parameters between the working and protection paths. In distance-diverse networks, the working and protection routes of a demand can be sufficiently different in terms of transmission conditions. Instead of enforcing the same transmission parameters for both routes, it was proposed to assign transmission parameters individually according to the specific conditions of each route.

The complexity of the routing and spectrum allocation (RSA) problem in a survivable elastic optical network is studied in [34] taking into account joint optimization of static unicast and anycast traffic demands in order to minimize the maximum spectrum usage. Moreover, different protection schemes are applied, namely, DPP and shared backup path protection (SBPP). Several works [35], [36] have investigated routing, modulation level and spectrum allocation (RMSA) problems. Further, [37], [38], and [39] studied RMSA problems with survivability over EON. For instance, the work in [37] investigated survivable EONs with multiclass traffic demand. The authors addressed the problem of RMSA and proposed a number of heuristic algorithms for path selection and resource allocation.

III. SYSTEM MODEL

A. PROBLEM STATEMENT AND FORMULATION

In this section, we formulate the problem of RAN function placement over wavelength division multiplexing/optical transport networks (WDM/OTNs) metro-aggregation with reliable slicing against link failures. We focus on reliable slicing with SLP in which multiple links share the same backup resources; reducing the amount of resources required for protection. The problem involves mapping of logical nodes composing the slice requests (SRs) over physical network nodes and mapping of virtual links over physical network links.

We consider a physical network topology modelled by an unweighted directed graph $\mathcal{G}_p(\mathcal{N}_p, \mathcal{E}_p)$, where $\mathcal{N}_p$ and $\mathcal{E}_p$ represent the sets of substrate metro nodes and bidirectional optical fiber links, respectively. Each metro node is featured with C_n computational capacity, while each direction has one optical fiber link with N_w wavelength channels each with capacity B. We assume that each SR is modelled by a virtual network graph $\mathcal{G}_v(\mathcal{N}_v, \mathcal{E}_v)$, where $\mathcal{N}_v$ and $\mathcal{E}_v$ represent the virtual nodes and virtual links, respectively. N_s represents set of all slice requests. We consider a three-layer RAN architecture, where RAN functions are split into RU, DU and CU. The core network is represented by user plane function (UPF).

Traditionally, a metro network has hierarchical infrastructure comprising (i) cell sites (CSs), (ii) access Central Offices (COs) and (iii) core COs. Firstly, CSs, which are responsible for RU functions, are randomly distributed to collect traffic from different user equipment (UEs) and then connect them to higher network stages, i.e. access and core COs. Secondly, access COs, which form the interface between CSs and core COs, are able to host both DU and CU functionalities. Finally, core COs, which act as the interface to the data network, are responsible for hosting UPF functions. In this paper, we utilize two different RAN deployment scenarios; VNE and SFC. In VNE, DU and CU functions within the same SR cannot be co-located on the same physical node. While in SFC, DU and CU functions belonging to the same SR are co-located on the same physical node. Fig. 1 illustrates an example of a substrate network assuming 3 SRs, where SRs 1 and 2 are deployed with VNE scenario. SR 3 is deployed with SFC scenario, where both DU and CU functions are co-located on the same access CO node (i.e. node 5).

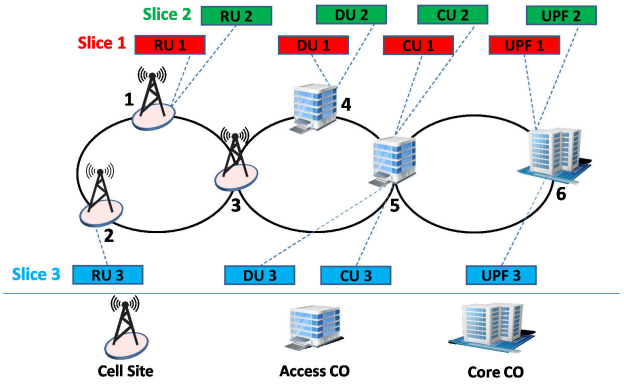

FIGURE 1. Network Architecture.

In this paper, we aim to achieve efficient VNF placement of virtual RAN functions over physical network nodes. In addition, we aim to achieve efficient primary and backup virtual link placement over physical links to protect against link failures using the SLP scheme to reduce backup resources. This ensures that a single link failure cannot disrupt the service. This is done using an efficient algorithm aiming to minimize the number of active wavelength channels. We also provide the optimization objective and constraints to formulate the problem of survivable slicing using SLP. The problem involves node mapping and link mapping constraints for working and backup links. Eq. (1) shows the optimization objective function that aims to minimize the number of wavelength channels utilized by both the working and backup lightpaths, where H_{ef}^{xy} and V_{ef}^{xy} are the numbers of primary and backup lightpaths between physical nodes x and y passes through link (e,f), respectively. All parameters and variables used in the problem formulation are listed in Tables 1 and 2, respectively.

Objective Function

$$Minmize \sum_{e,f \in N_p} \sum_{x,y \in N_p} H_{ef}^{xy} + V_{ef}^{xy} \quad (1)$$

TABLE 1. List of parameters.

Parameter	Description
N_w	Number of wavelength channels per fiber link.
B	Capacity of each fiber link.
C_n	Computational capacity of physical node n.
C	Virtual network function required capacity.
S	Maximum allowable number of sharing links.

TABLE 2. List of variables.

Variables	Description
η^j_{un}	1 if virtual function u of slice request j is mapped on physical node n.
H^{xy}_{ef}	Number of primary lightpaths between physical nodes x and y passes through link (e,f).
$\hat{H}^{xy}_{ef}$	1 if at least one primary ligthpath between physical nodes x and y passes through link (e,f).
V^{xy}_{ef}	Number of backup lightpaths between physical nodes x and y passes through link (e,f).
$\hat{V}^{xy}_{ef}$	1 if at least one backup ligthpath between physical nodes x and y passes through link (e,f).
A_{xy}	Number of lightpaths between physical nodes x and y.

Node Constraints

$$\sum_{n\in N_p} \eta^j_{un} = 1 \qquad \forall\, u \in N_v, j \in N_s \tag{2}$$

$$\sum_{u\in N_v, j\in N_s} \eta^j_{un} \times C \le C_n \qquad \forall\, n \in N_p \tag{3}$$

Link Constraints

$$\sum_{\substack{f\in Np\\ f\neq e}} H^{xy}_{ef} - \sum_{\substack{f\in Np\\ f\neq e}} H^{xy}_{fe} = \begin{cases} A_{xy}, & e = x \\ -A_{xy}, & e = y \\ 0, & \text{otherwise} \end{cases} \qquad \forall\, e, x, y \in N_p \tag{4}$$

$$\sum_{\substack{f\in Np\\ f\neq e}} V^{xy}_{ef} - \sum_{\substack{f\in Np\\ f\neq e}} V^{xy}_{fe} = \begin{cases} A_{xy}, & e = x \\ -A_{xy}, & e = y \\ 0, & \text{otherwise} \end{cases} \qquad \forall\, e, x, y \in N_p \tag{5}$$

$$\hat{H}^{xy}_{ef} + \hat{H}^{xy}_{fe} + \hat{V}^{xy}_{ef} + \hat{V}^{xy}_{fe} \le 1 \tag{6}$$

$$\sum_{x,y\in N_p} R(H^{xy}_{ef} + \frac{V^{xy}_{ef}}{S}) \le N_w \times B \qquad \forall\, e, f \in N_p \tag{7}$$

The constraint in Eq. (2) ensures that the virtual function u of slice request j is mapped to a single physical node. The constraint in Eq. (3) ensures that the capacity of all virtual functions mapped to a physical node is less than or equal to the physical node's available capacity. Eqs. (4) and (5) ensure flow conservation constraints for primary and backup links, respectively. Eq. (6) ensures that the lightpath moving from physical link x to y through link (e,f) is not moving in the opposite direction. In addition it guarantees the link disjointness between working and backup paths. Based on Eq. (7) a fiber link's working and shared backup lightpaths cannot have a combined wavelength capacity exceeding the total link capacity.

B. SLICE REQUIREMENT

Slices of the network refer to different functions and connections tailored to a particular performance and service requirements. The set of VNFs that make up a slice is represented by RU, DU, CU, and UPF.

We consider a network slice to be defined by its requirements in terms of the computational complexity of each VNF and the transport bandwidth. The computational complexity of a VNF, mapped on a given physical node, should not exceed the maximum node capacity. The baseband function processing complexity is measured in Giga Operation Per Second (GOPS), which denotes the required VNF computational resources. In [40], the baseband processing chain of the DU function is modelled as a sequence of processing functions (PFs) PF_i, for $i = 1, \ldots, 6$. VNFs' required computational capacities are calculated by [14]

$$C_{RU} = G_1 + G_2, \tag{8}$$

$$C_{DU} = (G_3 + G_4 + G5) \times L + G_6, \tag{9}$$

$$C_{CU} = G_6, \tag{10}$$

$$C_{UPF} = G_6, \tag{11}$$

where G_i represents the computational complexity associated with PF_i while L represents the number of resource blocks dedicated to a slice.

The required transport bandwidth of the network depends on the deployed RAN scenario. In VNE, the transport infrastructure includes three connections between function pairs RU/DU, DU/CU and CU/UPF, fronthaul, midhaul, and backhaul, respectively. While in SFC, the transport infrastructure only includes fronthaul and backhaul connections, as midhaul connections are terminated inside the nodes.

Traditionally, the amount of bandwidth used is determined by the traffic flow of a given network connection. In link protection, the optimal bandwidth allocation can be regarded as a classical routing and wavelength assignment (RWA) problem, where the total bandwidth resources required for primary and backup links should not exceed the total link capacity, $L_{cap} = C_{cap} - U_{cap}$, where L_{cap} is the available link capacity, C_{cap} is the total link capacity and U_{cap} is the used link capacity for primary and backup resources. The bandwidth requirements for fronthaul, midhaul and backhaul connections are computed by [14]

$$R_F = (N_{sc} \times N_{sym} \times N_{lay} \times S_{iq} \times 2 + O_{phy}) \times \frac{L}{L_{ref}}, \tag{12}$$

$$R_M = R_p + Opr, \tag{13}$$

$$R_B = R_p. \tag{14}$$

There are a number of considerations that should be taken into account when calculating the transport bandwidth requirements of a 5G network. These considerations include

number of subcarriers N_{sc}, number of symbols per millisecond N_{sym}, number of multiple input-multiple output (MIMO) layers N_{lay}, number of bits per sample S_{iq}, physical layer overhead O_{phy}, 5G peak data rate R_p, packet data convergence protocol- radio link control (PDCP-RLC) overhead O_{pr}, number of physical resource blocks (PRBs) L_{ref} and number of physical resource blocks dedicated to the slice L. Since each slice has its own requirements for computational complexity, transport bandwidth and isolation, it is more complex and challenging to share backup resources in a sliced optical network compared to backup sharing in traditional WDM networks.

C. RELIABLE SLICING WITH SLP

The complexity of SLP is higher than that of DLP as it involves a multiplexing process of multiple links, which are not expected to fail simultaneously, to share the same backup resources. However, SLP is introduced to ensure slice reliability against link failures with reduced backup resource usage in comparison to DLP. In this subsection, we show the wavelength channel utilization technique for both DLP and SLP in terms of backup resource usage.

In Fig. 2, we show how wavelength channels are assigned for both primary and backup links in case of DLP and SLP. We assume a physical network topology with 6 nodes and 9 links, where each physical link has 5 wavelength channels. We assume 4 SRs; primary links of slice 1 and 2 are mapped to link 4 [see Fig. 2(a)], while their corresponding backup links are mapped to links 3 and 5 (i.e. link-disjoint) [see Fig. 2(b)]. Primary link of slice 3 is mapped to link 6, while its corresponding backup links are mapped to links 5 and 7. For slice 4, primary link is mapped to link 5, while its corresponding backup links are mapped to links 3 and 4.

In DLP, each primary link requires dedicated backup resources for protection on backup links with the same capacity as the primary link. Accordingly, we assume that each SR requires one wavelength channel to be assigned on the primary link [see Fig. 2(c)] and one wavelength channel on each of the backup links [see Fig. 2(d)]. On the other hand, in SLP, multiple links are allowed to share the same backup resources. Hence, as an example, if link 6 fails, the required backup of link 6 on link 5 will be shared with the already reserved capacity for the primary link 4, i.e. no new backup capacity will be reserved on link 5 for link 6's protection, [see Fig. 2(e)]. Whereas on link 7, a new backup capacity will be reserved as there is no previously reserved protection capacity to be shared from other links. Similarly, if link 5 fails, the required backup of link 5 on link 3 will be shared with the already reserved capacity for the primary link 4, i.e. no new backup capacity will be reserved on link 3 for link 5's protection, [see Fig. 2(e)]. Whereas on link 4, a new backup capacity will be reserved as there is no previously reserved protection capacity to be shared from other links. Eventually, for the presented example with 4 SRs, 8 and 6 backup resources are reserved for DLP and SLP backup links, respectively, as shown in Figs. 2(d) and 2(e).

TABLE 3. Mapping example of 100 SRs on physical links.

Primary links	SRs	Required capacity	Backup links
1	10	10R	2, 3
2	20	20R	1, 3
3	15	15R	4, 5
4	20	20R	3, 5
5	5	5R	3, 4
6	30	30R	5, 6
⋮	⋮	⋮	⋮

Here, we extend the mapping problem to be represented by *mapping matrices*. *Mapping matrices* are classified into three matrices; primary link mapping matrix $\mathbf{X}$, primary link required protection capacity matrix $\mathbf{Y}$ and reserved backup capacity matrix $\mathbf{Z}$. $\mathbf{X}$ defines the mapping of primary link lp_i^j, where i refers to primary link number of a given network connection of SR j, on a set of link-disjoint backup path $\overline{\mathcal{LB}}_i = \{lb_i^1, lb_i^2, lb_i^3, \ldots, lb_i^m, \ldots\}$, where m refers to backup link number. Whereas $\mathbf{Y}$ and $\mathbf{Z}$ define the required and the reserved protection capacity on each backup link, respectively. The dimensions of these *mapping matrices* are determined by the number of physical links within the network and the number of bundles. Each bundle $\mathcal{B}_n = \{B_n^1, B_n^2, B_n^3, \ldots, B_n^s, \ldots\}$ refers to s sharing links, where n is the bundle number, $s \in \{1, \ldots, S\}$ is the mapping slot location within bundle n and S is the maximum allowable number of sharing links for a given bundle. The mapping location of primary link lp_i^j on a backup link lb_i^m is indicated by B_n^s.

In Table 3, we provide an illustrative example for the mapping of 100 SRs. We assume that we have 10, 20, 15, 20, 5 and 30 SRs mapped to primary links 1, 2, 3, 4, 5 and 6, respectively. Each SR requires a capacity of R on the mapped primary link. For the given network topology in Fig.2, we associate each primary link with a link-disjoint path (backup links) in order to ensure survivability against link failure.

Fig. 3 shows SLP *mapping matrices* where we assume $S = 2$ (i.e. each two primary links share the same backup capacity). According to Table 3, the primary links of 10 SRs are mapped to link 1 (i.e. lp_i^j=lp_1^j) and their corresponding backup links are mapped to links 2 and 3 (i.e $\overline{\mathcal{LB}}_1 = \{lb_1^2, lb_1^3\}$), requiring a capacity of $10R$ on each of the backup links. $\mathbf{X}$ is updated as $\mathbf{X}(m, B_n^s) = i$. Consequently, $\mathbf{X}(2, B_1^1) = 1$ and $\mathbf{X}(3, B_1^1) = 1$. $\mathbf{Y}$ is updated as $\mathbf{Y}(2, B_1^1) = 10R$ and $\mathbf{Y}(3, B_1^1) = 10R$.

Similarly, the primary links of 20 SRs are mapped to link 2 (i.e. $lp_i^j = lp_2^j$) and their corresponding backup links are mapped to links 1 and 3 (i.e. $\overline{\mathcal{LB}}_2 = \{lb_2^1, lb_2^3\}$), requiring a capacity of $20R$ on each of the backup links. In this case, $\mathbf{X}$ is updated as $\mathbf{X}(1, B_1^1) = 2$ and $\mathbf{X}(3, B_1^2) = 2$. $\mathbf{Y}$ is updated as $\mathbf{Y}(1, B_1^1) = 20R$ and $\mathbf{Y}(3, B_1^2) = 20R$. To define the reserved backup capacity on each backup link, we first get the required capacity of each bundle as the maximum capacity required by the sharing links of the bundle. Then, we calculate the

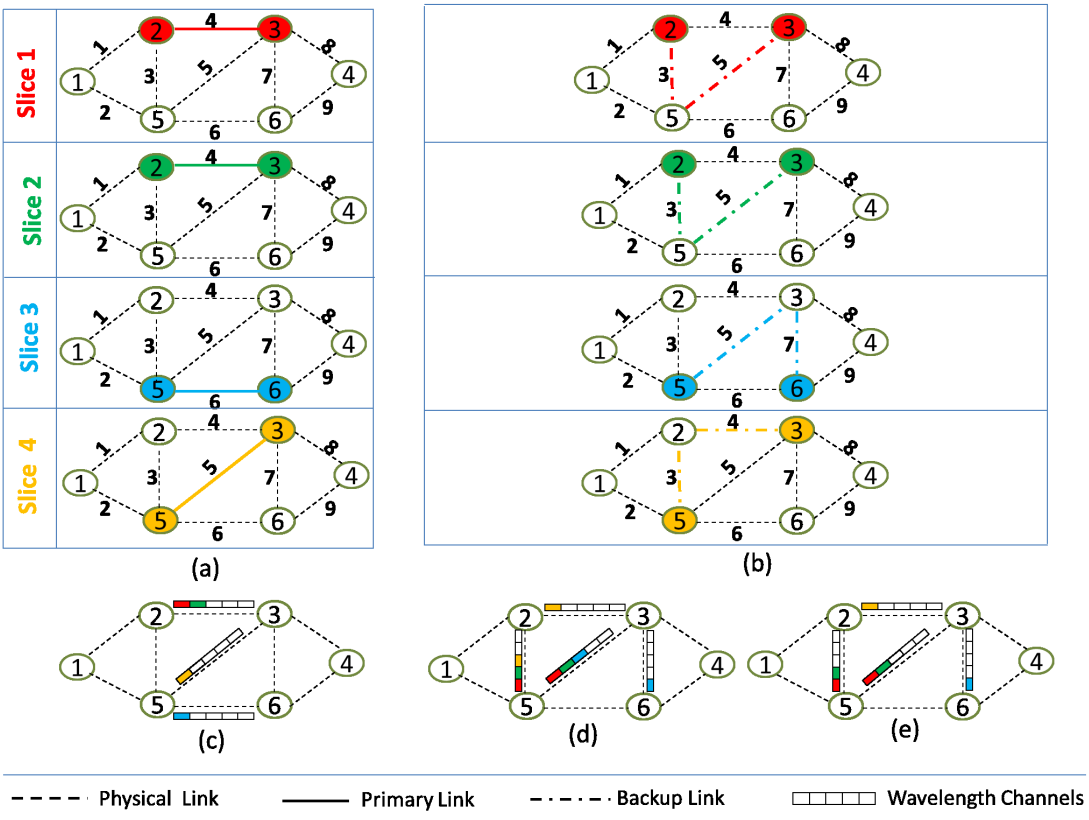

FIGURE 2. Link mapping for (a) primary link, (b) backup link. Wavelength channel assignment for (c) primary link, (d) backup link in case of DLP and (e) backup link in case of SLP.

total reserved backup capacity on each backup link as the summation of the required capacity of all bundles. In our example, the reserved backup capacity on link 3 for the two sharing primary links 1 and 2 (i.e. bundle 1) is the capacity of the sharing link with the highest required backup capacity; that is, link 2 in this case. Therefore, $\mathbf{Z}(3, B_1) = 20R$. The remaining SRs in the example are mapped using the same approach as described above.

After mapping of all the SRs in the given example of Table 3. To further illustrate the different cases that the proposed SLP algorithm handles, assume 15 new SRs are assigned to primary link 4 with a new required capacity of $15R$. The backup on link 3 will be mapped to B_2^1 (i.e. the previously mapped location of primary link 4 on backup link 3 from previous SRs). Therefore, the reserved capacity for B_2 will increase from $20R$ to $35R$, $\mathbf{Z}(3, B_2) = 35R$. For the backup on link 5, if we map it on $\mathbf{X}(5, B_1^2)$ (i.e. the previously mapped location), the reserved capacity for B_1 will increase from $30R$ to $35R$, $\mathbf{Z}(5, B_1) = 35R$. However, B_2 has an empty mapping slot B_2^2 in this case. If we map link 4 on $\mathbf{X}(5, B_2^2)$, no new extra capacity will be reserved for B_2 as it will be shared with the reserved backup capacity of primary link 3. Using this approach, our proposed algorithm determines the most appropriate mapping location that provides the minimal amount of additional required backup capacity.

IV. ALGORITHM DESCRIPTION

A. NODE MAPPING ALGORITHM

The presented node mapping algorithm addresses the problem of RAN function placement with the objective of minimizing the number of physical links hosting virtual links. The given bi-directional graph, representing the physical network, is constructed by the use of a binary *connectivity matrix*. A *connectivity matrix* is defined as a square matrix with the size of the total number of nodes in the network. Each cell in the matrix represents a connection between two nodes. Each cell with value 1 refers to a direct connection between two nodes, while a value of 0 refers to no connection. We assume that the given SRs are randomly generated at different CS nodes which are considered as the source nodes. RU functions are consequently mapped on the source CS nodes. The node mapping algorithm is devised in Algorithm 1.

For a given SR, originating from a certain CS node, RU function is mapped if the required RU function capacity is less than or equal to the residual node capacity of source node q. Initially, the algorithm maps the UPF function to the nearest core CO node (steps 4 to 10 in Algorithm 1). The distance d_{qt} from the source node q to each core CO node $t \in \overline{\mathcal{N}}_c$ is calculated; where $\overline{\mathcal{N}}_c$ is a set of all core COs nodes in the network. Next, we perform end node ranking from nearest to farthest, according to d_{qt}, so that the aim

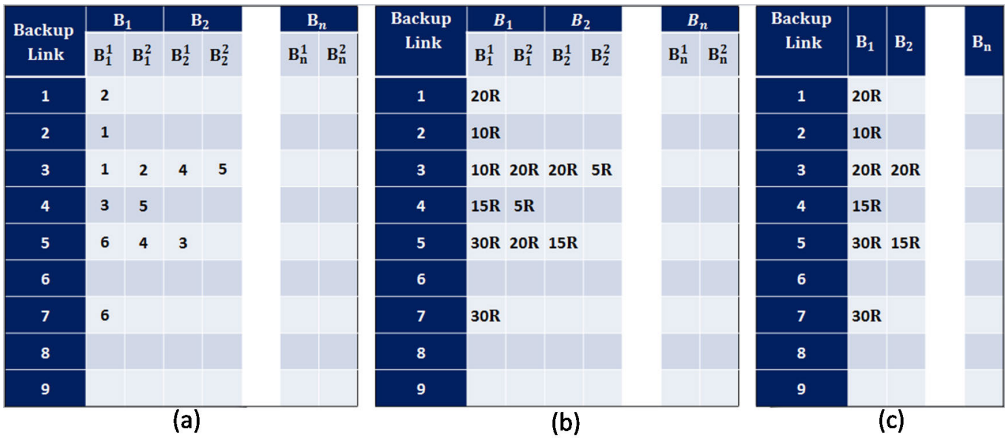

Backup Link	B_1		B_2		B_n	
	B_1^1	B_1^2	B_2^1	B_2^2	B_n^1	B_n^2
1	2					
2	1					
3	1	2	4	5		
4	3	5				
5	6	4	3			
6						
7	6					
8						
9						

(a)

Backup Link	B_1		B_2		B_n	
	B_1^1	B_1^2	B_2^1	B_2^2	B_n^1	B_n^2
1	20R					
2	10R					
3	10R	20R	20R	5R		
4	15R	5R				
5	30R	20R	15R			
6						
7	30R					
8						
9						

(b)

Backup Link	B_1	B_2	B_n
1	20R		
2	10R		
3	20R	20R	
4	15R		
5	30R	15R	
6			
7	30R		
8			
9			

(c)

FIGURE 3. SLP *mapping matrices* with $S = 2$ (a) primary link mapping matrix X, (b) primary link required capacity matrix Y, (c) reserved backup capacity matrix Z.

Algorithm 1 Node Mapping

Input: Connectivity graph $\mathcal{G}_p(\mathcal{N}_p, \mathcal{E}_p)$, C_{RU}, C_{DU}, C_{CU} and C_{UPF}.

Output: RAN function placement.

1: **for** each SR **do**
2: **if** $C_{RU} \leq C_{q_{res}}$ **then**
3: map RU function on physical node q.
4: calculate distance d_{qt} between source node q and each core CO node $t \in \overline{\mathcal{N}}_c$.
5: $\overline{\mathcal{D}} \leftarrow$ sorted core CO nodes from nearest to farthest.
6: $r \leftarrow 1$.
7: **while** $C_{UPF} > C_{\overline{\mathcal{D}}(r)_{res}}$ and $r \leq |\overline{\mathcal{D}}|$ **do**
8: $r \leftarrow r + 1$.
9: **end while**
10: map UPF function on physical node $\overline{\mathcal{D}}(r)$.
11: calculate k-shortest paths from q to $\overline{\mathcal{D}}(r)$ and store paths in $\overline{\mathcal{P}}$.
12: for VNE, choose the shortest path from $\overline{\mathcal{P}}$ containing at least one node with $C_{DU} \leq C_{n_{res}}$ and at least one node with $C_{CU} \leq C_{n_{res}}$.
for SFC, choose the shortest path from $\overline{\mathcal{P}}$ containing at least one node with $C_{DU} + C_{CU} \leq C_{n_{res}}$.
13: if all functions are mapped, then set η_n=1.
14: update residual node capacities $C_{n_{res}}$.
15: **else**
16: η_n=0.
17: **end if**
18: **end for**

of minimizing the number of physical links hosting virtual links can be achieved. Ranked nodes are stored in $\overline{\mathcal{D}}$. The algorithm finds the nearest core node in $\overline{\mathcal{D}}$ with enough capacity for mapping the UPF function. If the UPF function is mapped, the algorithm starts to map both DU and CU functions according to the required deployment strategy (steps 11 and 12 in Algorithm 1). According to the problem statement, the algorithm finds the shortest path from source node q to destination node $\overline{\mathcal{D}}(r)$ so that the number of physical links is minimized, where r is the index of the nearest core CO node with enough capacity for mapping the UPF function. We calculate k-shortest paths using Dijkstra's algorithm and store all paths in $\overline{\mathcal{P}}$.

For the VNE deployment strategy, the algorithm chooses the shortest path from $\overline{\mathcal{P}}$ containing at least one physical node n with enough residual node capacity, $C_{n_{res}}$, to host the DU function which requires capacity, C_{DU}, and at least another physical node with enough residual node capacity to host the CU function with required capacity C_{CU}. While in case of SFC, the DU and CU functions are co-located on the same node. Hence, the algorithm chooses the shortest path from $\overline{\mathcal{P}}$ containing at least one node with enough capacity for hosting both DU and CU functions. Finally, if all functions are mapped, we set the node mapping flag η_n to 1 and update the residual capacity of mapped nodes.

B. SLP MAPPING ALGORITHM

There are two key challenges for any SLP scheme; namely, determining the amount of backup resources and determining which links will be multiplexed to share the same backup resources. In this subsection, we propose an efficient mapping solution to associate primary links with their corresponding backup links. The algorithm identifies the primary links that can share backup resources such that the number of backup wavelength channels is reduced. The objective of this algorithm is to update the SLP *mapping matrices* (described in Section III-C). The SLP mapping algorithm is devised in Algorithm 2.

The algorithm takes as input the primary link lp_i^j and an element of its corresponding backup path $\overline{\mathcal{LB}}_i$ (these inputs are created using Algorithm 3 and will be discussed later). The algorithm aims to map lp_i^j on each of the backup links in $\overline{\mathcal{LB}}_i$ and to decide the required sharing capacity to be reserved

Algorithm 2 SLP Mapping

Input: lp_i^j, lb_i^m, R.

Output: update SLP *mapping matrices* **X**, **Y** and **Z**.

1: **Condition 1**: lp_i^j is not previously mapped to lb_i^m, and no active bundle or all bundles are fully occupied.
2: activate new bundle and update **X**, **Y** and **Z** matrices

$$\mathbf{X}(m, B_n^1) \leftarrow i, \tag{15}$$
$$\mathbf{Y}(m, B_n^1) \leftarrow R, \tag{16}$$
$$\mathbf{Z}(m, \mathcal{B}_n) \leftarrow R. \tag{17}$$

3: **Condition 2**: lp_i^j is not previously mapped to lb_i^m, and there is a bundle with an empty mapping slot.
4: $B_n^e \leftarrow$ first empty mapping slot location.
5: update **X**, **Y** and **Z** matrices

$$\mathbf{X}(m, B_n^e) \leftarrow i, \tag{18}$$
$$\mathbf{Y}(m, B_n^e) \leftarrow R, \tag{19}$$
$$\mathbf{Z}(m, \mathcal{B}_n) \leftarrow \max_{s\in\{1,\ldots,S\}} \mathbf{Y}(m, B_n^s). \tag{20}$$

6: **Condition 3**: lp_i^j is previously mapped to lb_i^m at only one location in a bundle with an empty mapping slot.
7: $B_n^s \leftarrow i$ mapped location on $\mathbf{X}(m)$.
8: update **Y** as

$$\mathbf{Y}(m, B_n^s) \leftarrow \mathbf{Y}(m, B_n^s) + R. \tag{21}$$

9: update **Z** according to (20).
10: **Condition 4**: lp_i^j is previously mapped to lb_i^m at several locations, and all bundles are fully occupied or there is a bundle with an empty mapping slot that contains lp_i^j.
11: $\overline{\mathcal{Q}} \leftarrow i$ mapped locations on $\mathbf{X}(m)$.
12: $B_{n_{min}}^s \leftarrow$ bundle location in $\overline{\mathcal{Q}}$ providing minimum additional required backup capacity.
13: update **Y** as

$$\mathbf{Y}(m, B_{n_{min}}^s) \leftarrow \mathbf{Y}(m, B_{n_{min}}^s) + R. \tag{22}$$

14: update **Z** according to (20).
15: **Condition 5**: lp_i^j is previously mapped to lb_i^m at several locations, and there is a bundle with an empty mapping slot that does not contain lp_i^j.
16: perform steps 4 and 11.
17: add B_n^e to mapping location set $\overline{\mathcal{Q}}$.
18: perform steps 12 to 14.

on each backup link. The algorithm defines five mapping conditions, according to the existence of lp_i^j in matrix **X** and according to bundle occupation (i.e. if any bundle has empty mapping slots or not). It is worthwhile to mention that lp_i^j can be mapped several times on the same backup link lb_i^m, but at different bundles. Our proposed algorithm chooses the most appropriate bundle location that provides the minimal amount of additional required backup capacity for the current lp_i^j mapping.

Condition 1 refers to the case when lp_i^j is not previously mapped to lb_i^m, and no active bundle or all bundles are fully occupied. In this case, we activate a new bundle to map lp_i^j on backup link lb_i^m at the first mapping slot location B_n^1. Afterwards, **X**, **Y** and **Z** are updated according to Eqs. (15) - (17). Then, lp_i^j is mapped to the newly created bundle with no other sharing links. Accordingly, for this bundle $\mathcal{B}_n$, both **Y** and **Z** matrices are updated by R.

Similarly, in condition 2, lp_i^j is not previously mapped to lb_i^m, however, there is an active bundle with an empty mapping slot. Therefore, the algorithm maps lp_i^j to the first empty mapping slot location B_n^e. Then, **X**, **Y** and **Z** are updated according to Eqs. (18)- (20). For this bundle $\mathcal{B}_n$, $\mathbf{Y}(m, B_n^e)$ is updated as R, while **Z** is updated by the maximum required capacity from all the sharing links of this bundle.

In condition 3, the algorithm checks if lp_i^j is previously mapped to lb_i^m at only one location in a bundle that consists of an empty mapping slot. In this case, the required capacity R will be added to the previous required capacity of lp_i^j in **Y**. **Y** and **Z** are then updated according to Eqs. (21) and (20), respectively.

In condition 4, where lp_i^j is previously mapped to lb_i^m at several locations, and all bundles are fully occupied or there is a bundle with an empty mapping slot that contains lp_i^j.

Firstly, for the given backup link lb_i^m, the algorithm finds all lp_i^j bundle mapped locations in $\mathbf{X}(m)$ and stores them in the mapping location set $\overline{\mathcal{Q}}$.

In step 12, we find the bundle location that provides the minimal amount of additional required backup capacity for the current lp_i^j mapping $B_{n_{min}}^s$. Finally, after deciding the most appropriate mapping location $B_{n_{min}}^s$, the original *mapping matrices* **Y** and **Z** are updated according to Eqs.(22) and (20), respectively.

In condition 5, where lp_i^j is previously mapped to lb_i^m at several locations, and there is a bundle with an empty mapping slot that does not contain lp_i^j. We perform steps 4 and 11 to find the first empty mapping slot location as well as lp_i^j previously mapped locations on $\mathbf{X}(m)$. In step 17, B_n^e is added to the mapping location set $\overline{\mathcal{Q}}$. Afterwards, we perform steps 12 to 14 to update Y and Z.

C. LINK MAPPING ALGORITHM

The objective of this algorithm is to find efficient virtual link mapping for both primary and backup links when considering the SLP scheme. The primary goal is to achieve minimum wavelength channel usage. The link mapping algorithm is executed only if all VNF functions are mapped for a given SR (i.e. node mapping flag $\eta_n = 1$). To map virtual links, the algorithm finds the shortest path between VNF mapped nodes (i.e. RU/DU, DU/CU, and CU/UPF nodes). As part of our

node mapping algorithm, we use a k-shortest path algorithm with a proper value for k so that all VNFs are mapped. The algorithm iterates on k-shortest paths until mapping of all VNFs occurs for a given SR.

In practice, choosing the shortest path might not always result in a feasible solution for link mapping with SLP. The reason is that the capacity of each of the shortest path links and their corresponding link-disjoint paths might not be sufficient for mapping primary and backup links. Further, determining a suitable value of k in a k-shortest path algorithm for link mapping with SLP is affected by several factors. In fact, the required backup capacity of a given primary link on a backup link varies, for a shared protection strategy, depending on the previously mapped primary links on the given backup link and the available empty slots on the bundles of that backup link. As a result, the numerous cases described in the SLP mapping algorithm impose a more involved approach when designing the link mapping algorithm. For that purpose, we devise a constrained auxiliary graph instead of using the input connectivity graph for shortest path selection. Based on this auxiliary graph, we set $k = 1$ and obtain the shortest path along the auxiliary graph, which corresponds to the most efficient path in terms of wavelength channel usage. The link mapping algorithm is devised in Algorithm 3. The details of the construction of the auxiliary graph are discussed in the following.

Initially, for each connection (i.e. fronthaul, midhaul and backhaul), the required primary link capacity R is calculated according to Eqs. (12) to (14). In step 4, the above mentioned constraints of the auxiliary graph are illustrated. For the given connectivity graph $\mathcal{G}_p(\mathcal{N}_p, \mathcal{E}_p)$, the algorithm finds links in $\mathcal{E}_p$ with capacity greater than or equal to the required primary link capacity R and adds them to the set $\overline{\mathcal{L}}_a$. For links in $\overline{\mathcal{L}}_a$, the algorithm finds links with available link-disjoint path having enough capacity for shared protection and adds them to the set $\overline{\mathcal{L}}_b$. To illustrate, the algorithm loops on each link in $\overline{\mathcal{L}}_a$ being regarded as a primary link. Then, using Algorithm 2 for the given primary link and considering the rest of the links in $\mathcal{E}_p$ for backup protection, the algorithm attempts to find a link-disjoint path having enough shared protection capacity. If no such path exists, this primary link is removed from $\overline{\mathcal{L}}_a$. Finally, the remaining links are added to the set $\overline{\mathcal{L}}_b$, i.e., the set of all feasible links for the current primary link mapping.

In step 7, the auxiliary graph is constructed by the use of an auxiliary *connectivity matrix* considering only the links in $\overline{\mathcal{L}}_b$. After graph construction, the shortest path between virtual link end nodes is determined. According to the connectivity graph and RAN function placement, a primary link for a given network connection might be more than one physical link. Primary links generated from the shortest path in step 8 are indicated by $\overline{\mathcal{LP}} = \{lp_1, lp_2, lp_3, \ldots, lp_i\}$, where i here refers to primary link number. For each link in $\overline{\mathcal{L}}_p$, the physical link available capacity of lp_i^j is updated.

The above auxiliary graph is not efficient for backup path selection. This is because it does not contain links with capacity less than the required primary link capacity R. However, a link may not have enough capacity to handle the virtual link's required capacity R, but can still be used as a backup link and share backup resources. Therefore, in steps 11 to 18, we find links $\overline{\mathcal{L}}_y$ to generate a new auxiliary graph for backup path selection. In step 11, all links in $\mathcal{E}_p$ except lp_i^j are stored in $\overline{\mathcal{L}}_x$. Initially we set $\overline{\mathcal{L}}_y$ to be equal to $\overline{\mathcal{L}}_x$. For each link in $\overline{\mathcal{L}}_x$, we get the required sharing capacity using Algorithm 2 with inputs lp_i^j and $lb_i^m = l_{xv}$, where v is an index for links in $\overline{\mathcal{L}}_x$. If the required sharing capacity on l_{xv} is greater than the available link capacity, l_{xv} is removed and the rest of links are stored in $\overline{\mathcal{L}}_y$. In steps 19 and 20, a new auxiliary graph is constructed using the remaining links in $\overline{\mathcal{L}}_y$.

Algorithm 3 Link Mapping

Input: Connectivity graph $\mathcal{G}_p(\mathcal{N}_p, \mathcal{E}_p)$, R.
Output: Virtual link mapping for primary and backup links.

1: **for** each SR **do**
2: **for** each connection **do**
3: $R \leftarrow$ required link capacity.
4: for the given connectivity graph, find below constraints:
5: a. $\overline{\mathcal{L}}_a \leftarrow$ links in $\mathcal{E}_p$ with capacity $\geq R$.
6: b. $\overline{\mathcal{L}}_b \leftarrow$ links in $\overline{\mathcal{L}}_a$ with available link-disjoint path having enough shared protection capacity.
7: construct auxiliary graph for primary link selection considering links in $\overline{\mathcal{L}}_b$.
8: $\overline{\mathcal{L}}_p \leftarrow$ shortest path considering auxiliary graph generated in step 7.
9: **for** each link in $\overline{\mathcal{L}}_p$ **do**
10: update the available physical link capacity L_{cap} of lp_i^j.
11: $\overline{\mathcal{L}}_x \leftarrow \mathcal{E}_p \backslash \{lp_i\}$.
12: $\overline{\mathcal{L}}_y \leftarrow \overline{\mathcal{L}}_x$.
13: **for** each link $l_{xv} \in \overline{\mathcal{L}}_x$ **do**
14: get the required sharing capacity on l_{xv} using Algorithm 2 with inputs lp_i^j and $lb_i^m = l_{xv}$.
15: **if** the required sharing capacity on l_{xv} is greater than the available link capacity L_{cap}. **then**
16: $\overline{\mathcal{L}}_y \leftarrow \overline{\mathcal{L}}_y \backslash \{l_{xv}\}$.
17: **end if**
18: **end for**
19: construct auxiliary graph for backup link selection considering links in $\overline{\mathcal{L}}_y$.
20: $\overline{\mathcal{LB}}_i \leftarrow$ shortest path between end nodes of lp_i^j considering auxiliary graph generated in step 19.
21: **for** each link in $\overline{\mathcal{LB}}_i$ **do**
22: update *mapping matrices* $\mathbf{X}, \mathbf{Y}, \mathbf{Z}$ using Algorithm 2.
23: **end for**
24: **end for**
25: **end for**
26: **end for**

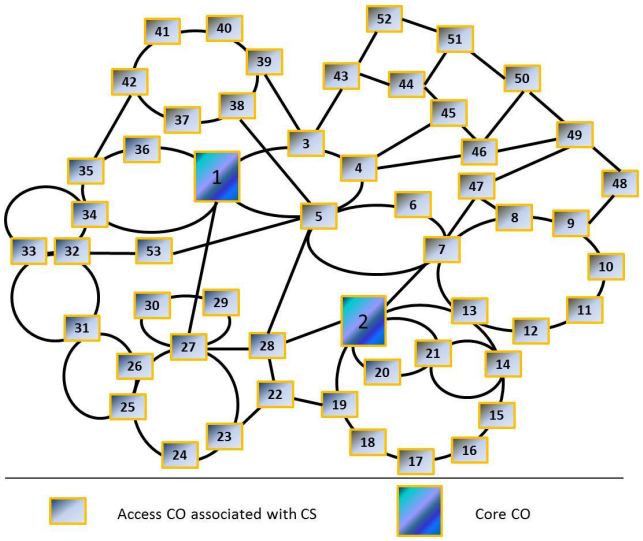

FIGURE 4. Large Scale Network Topology.

Then, the shortest path between end nodes of lp_i^j is selected as the backup links. The backup links for the primary link lp_i^j, generated in step 20, are denoted by the set $\overline{\mathcal{LB}}_i$. Finally, for each link in $\overline{\mathcal{LB}}_i$, we update the *mapping matrices* using Algorithm 2.

V. PERFORMANCE EVALUATION

A. SIMULATION SETUP

In this paper, simulation results are conducted with a radio configuration of 100 MHz system bandwidth, 256 QAM and 8 × 8 MIMO. According to this radio configuration, 500 resource blocks (RBs) are available in each CS. We assume that multiple SRs are allowed to share these 500 RBs in each CS. Therefore, the number of requested RBs of all the SRs belonging to one CS cannot exceed 500. We consider a 53-node topology shown in Fig. 4 with 51 access CO nodes, where each access CO is associated with a CS node, and 2 core CO nodes. Nodes are connected to each other through a bi-directional fiber link. Each direction has one fiber link with 40 wavelength channels each with 40 Gbps capacity. We consider unlimited node capacity for access and core CO nodes. VNFs computational capacity requirements for each SR are calculated according to Eqs. (8) to (11). According to the radio configuration, the transport bandwidth requirements for fronthaul, midhaul and backhaul are calculated according to Eqs. (12) to (14). We assume that VNFs for all SRs are fully isolated, where VNFs of a given SR cannot be shared with other SRs. For network isolation, we first study the case of soft network isolation, where a single wavelength channel can be shared among multiple SRs. Then, we study the case of hard network isolation, where a single wavelength channel is fully dedicated for a given SR. To solve our problem, we used MATLAB version *R*2014*a* on workstation equipped with 8 × 2 GHz processor and 32 Gbyte RAM.

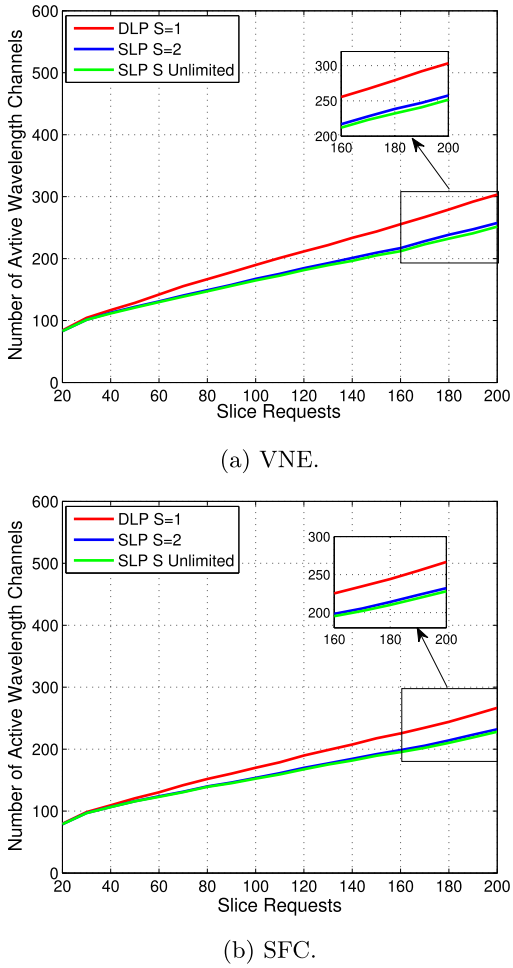

FIGURE 5. Wavelength channel utilization in the case of soft network isolation.

B. EVALUATION RESULTS

In this section, we compare the proposed SLP algorithm to the conventional model that adopts DLP [14]. In Fig. 5, the number of active wavelength channels for SLP relative to DLP scheme assuming soft network isolation is shown for the two deployment strategies; VNE and SFC. For SLP scheme, we first study the case when the number of sharing links S is unlimited, where all primary links that are mapped to a backup link share one backup resource unit. Then we study the case when S is set to 2, where each two primary links share one backup resource unit. It can be seen that there is a linear relationship between wavelength channel utilization and slice requests. SLP is shown to have better wavelength channel utilization than DLP by allowing lower backup resources especially for higher SRs. The difference between SLP when $S = 2$ and unlimited S is not significant for soft network isolation. This is due to the low probability of having more than two primary links that may share the same backup resources in the simulated large scale network. In other words, the probability of having more than two sharing primary links over the same protection link is low (e.g., in Fig. 3 (a) backup

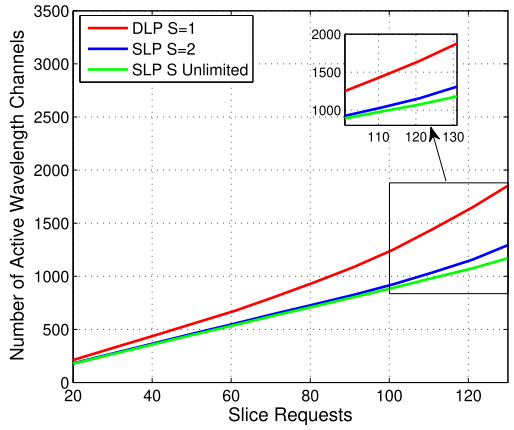

(a) VNE.

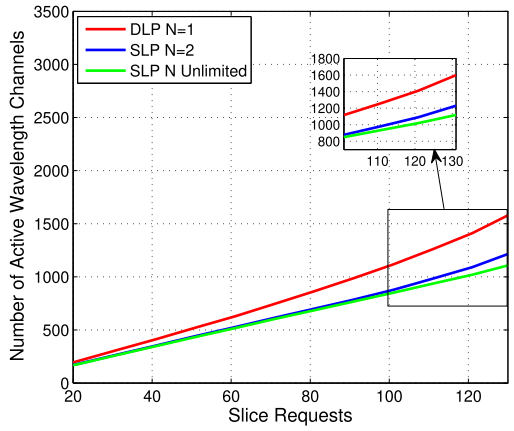

(b) SFC.

FIGURE 6. Wavelength channel utilization in the case of hard network isolation.

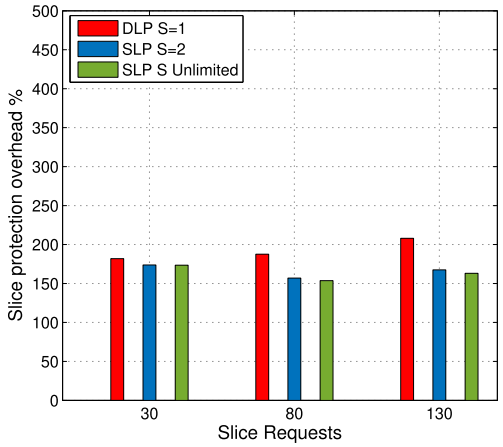

(a) Soft network isolation.

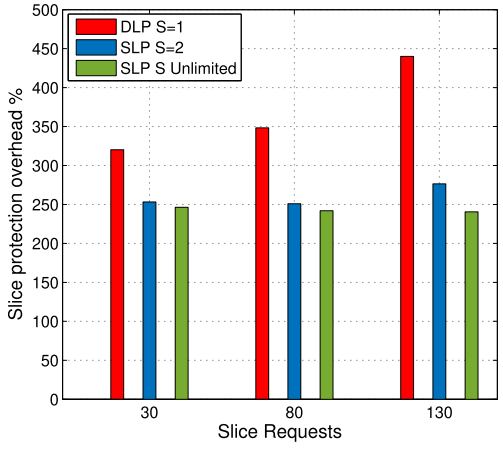

(b) Hard network isolation.

FIGURE 7. Slice protection overhead with VNE deployment strategy.

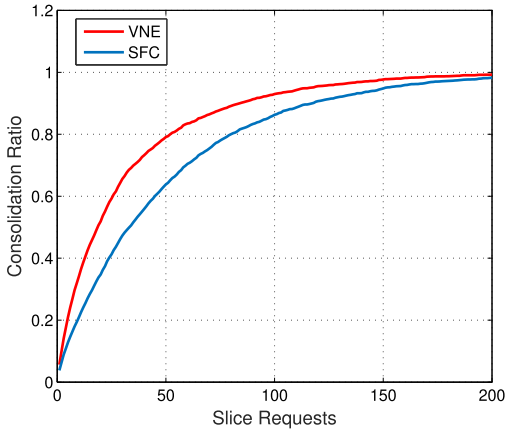

FIGURE 8. Consolidation Ratio.

link 3 has two bundles composed of four sharing primary links). While the probability of links with one bundle and only two sharing primary links is high (e.g., in Fig. 3 (a) backup link 4 with only one bundle and two sharing primary links). This reflects on the comparison between the case when S=2 and S=unlimited. As the percentage of backup links having more than two sharing primary links increases, the difference between the performance of SLP when S=2 and S=unlimited increases. As shown in Fig. 5(b) SFC is able to reduce wavelength channel utilization compared to VNE.

In Fig. 6, the number of active wavelength channels for SLP relative to DLP scheme assuming hard network isolation is shown for the two deployment strategies; VNE and SFC. It can be seen that wavelength channel utilization grows superlinearly with the number of slice requests, especially for DLP. In the case of hard network isolation, the superior performance of the proposed SLP scheme compared to the DLP scheme in terms of wavelength channel utilization is more significant than soft network isolation. For example, SLP is able to reduce backup resources by 15% and 37.7% at SR 130 for soft and hard isolations, respectively. This is due to the effect of using a dedicated wavelength channel for each SR and dedicated backup resources for DLP in case of hard network isolation. Alternatively, SLP with hard network isolation requires a dedicated wavelength channel for each SR, however, allowing backup resources to be shared among multiple links. This results in DLP having a much

higher blocking probability than SLP when the number of SRs increases beyond 130. This effect can be mitigated by the use of a weighted connectivity graph in order to prioritize the reuse of active links and minimize the number of newly activated ones. However, since our focus is to propose a more efficient link protection algorithm compared to the conventional DLP algorithm, we utilize an unweighted connectivity graph for the performance evaluation of both schemes. For hard network isolation, there is a slight difference between SLP when $S = 2$ and unlimited S, especially for higher SRs. In other words, the greater the likelihood of having more than two sharing primary links over the same protection link, the greater the difference between the performance of the case when S=2 and S=unlimited, which is seen for larger numbers of SRs. Note that the number of wavelength channels for hard network isolation is primarily affected by the number of mapped SRs. Similarly, in Fig. 6(b) SFC is able to reduce wavelength channel utilization compared to VNE.

Fig. 7 plots the slice protection overhead as the percentage of additional wavelength channels required for protection compared to the case without protection with the VNE deployment strategy. The protection overhead has superlinear behavior for DLP in the case of hard network isolation [see Fig. 7(b)], especially when the number of slice requests is high. SLP has a lower protection overhead than DLP for both soft and hard network isolations.

In Fig. 8, we show the consolidation ratio which represents the number of active nodes relative to the total number of nodes for the two deployment strategies; VNE and SFC. A lower consolidation ratio represents more consolidation (i.e. less nodes are activated to host RAN functions). The effect of co-locating DU and CU functions, in case of SFC, on the same node has the benefit of reducing the consolidation ratio leading to more efficient radio resources management.

VI. CONCLUSION

Providing high reliability services will be possible via slicing in future networks. In order to achieve this, a protection model with efficient resource management for primary and backup resources is required. In this paper, we investigate the virtual network embedding problem over elastic optical networks considering SLP in order to reduce the required backup resources. Our proposed heuristic algorithm is classified into node mapping, link mapping and SLP mapping. In the node and link mapping algorithms, we perform RAN function placement, and routing and wavelength assignment. The aim is to achieve minimum number of active wavelength channels. Our SLP mapping algorithm is represented by *mapping matrices* that define the mapping of S sharing primary links onto a given backup link. In addition, they also define the required and the reserved sharing capacity. Results show that SLP has the benefit of reduced backup resources compared to the conventional DLP model for the two deployment strategies VNE and SFC.

REFERENCES

[1] M. Chahbar, G. Diaz, A. Dandoush, C. Cérin, and K. Ghoumid, "A comprehensive survey on the E2E 5G network slicing model," *IEEE Trans. Netw. Service Manage.*, vol. 18, no. 1, pp. 49–62, Mar. 2021.
[2] N. M. M. K. Chowdhury and R. Boutaba, "A survey of network virtualization," *Comput. Netw.*, vol. 54, no. 5, pp. 862–876, Apr. 2010.
[3] L. Gong and Z. Zhu, "Virtual optical network embedding (VONE) over elastic optical networks," *J. Lightw. Technol.*, vol. 32, no. 3, pp. 450–460, Feb. 2014.
[4] N. Shahriar, S. Taeb, S. R. Chowdhury, M. Tornatore, R. Boutaba, J. Mitra, and M. Hemmati, "Achieving a fully-flexible virtual network embedding in elastic optical networks," in *Proc. IEEE INFOCOM Conf. Comput. Commun.*, Apr. 2019, pp. 1756–1764.
[5] S. Abdelwahab, B. Hamdaoui, M. Guizani, and T. Znati, "Network function virtualization in 5G," *IEEE Commun. Mag.*, vol. 54, no. 4, pp. 84–91, Apr. 2016.
[6] T. Chen, M. Matinmikko, X. Chen, X. Zhou, and P. Ahokangas, "Software defined mobile networks: Concept, survey, and research directions," *IEEE Commun. Mag.*, vol. 53, no. 11, pp. 126–133, Nov. 2015.
[7] Q. Duan, N. Ansari, and M. Toy, "Software-defined network virtualization: An architectural framework for integrating SDN and NFV for service provisioning in future networks," *IEEE Netw.*, vol. 30, no. 5, pp. 10–16, Sep. 2016.
[8] A. A. Barakabitze, A. Ahmad, R. Mijumbi, and A. Hines, "5G network slicing using SDN and NFV: A survey of taxonomy, architectures and future challenges," *Comput. Netw.*, vol. 167, Feb. 2020, Art. no. 106984.
[9] X. Foukas, G. Patounas, A. Elmokashfi, and M. K. Marina, "Network slicing in 5G: Survey and challenges," *IEEE Commun. Mag.*, vol. 55, no. 5, pp. 94–100, May 2017.
[10] H. Yu, F. Musumeci, J. Zhang, M. Tornatore, and Y. Ji, "Isolation-aware 5G RAN slice mapping over WDM metro-aggregation networks," *J. Lightw. Technol.*, vol. 38, no. 6, pp. 1125–1137, Mar. 15, 2020.
[11] I. Afolabi, T. Taleb, K. Samdanis, A. Ksentini, and H. Flinck, "Network slicing and softwarization: A survey on principles, enabling technologies, and solutions," *IEEE Commun. Surveys Tuts.*, vol. 20, no. 3, pp. 2429–2453, 3rd Quart., 2018.
[12] M. Ahsan, A. Ahmed, A. Al-Dweik, and A. Ahmad, "Functional split-aware optimal BBU placement for 5G cloud-RAN over WDM access/aggregation network," *IEEE Syst. J.*, vol. 17, no. 1, pp. 122–133, Mar. 2023.
[13] A. Marotta, D. Cassioli, M. Tornatore, Y. Hirota, Y. Awaji, and B. Mukherjee, "Reliable slicing with isolation in optical metro-aggregation networks," in *Proc. Opt. Fiber Commun. Conf. Exhib. (OFC)*, Mar. 2020, pp. 1–3.
[14] A. Marotta, D. Cassioli, M. Tornatore, Y. Hirota, Y. Awaji, and B. Mukherjee, "Multilayer protection-at-lightpath for reliable slicing with isolation in optical metro-aggregation networks," *J. Opt. Commun. Netw.*, vol. 14, no. 4, pp. 289–302, Apr. 2022.
[15] M. Liu, M. Tornatore, and B. Mukherjee, "Survivable traffic grooming in elastic optical networks-shared path protection," in *Proc. IEEE Int. Conf. Commun. (ICC)*, Jun. 2012, pp. 6230–6234.
[16] G. Le, S. Ferdousi, A. Marotta, S. Xu, Y. Hirota, Y. Awaji, M. Tornatore, and B. Mukherjee, "Survivable virtual network mapping with content connectivity against multiple link failures in optical metro networks," *J. Opt. Commun. Netw.*, vol. 12, no. 11, pp. 301–311, Nov. 2020.
[17] L. Song, J. Zhang, and B. Mukherjee, "Dynamic provisioning with availability guarantee for differentiated services in survivable mesh networks," *IEEE J. Sel. Areas Commun.*, vol. 25, no. 3, pp. 35–43, Apr. 2007.
[18] N. Shahriar, R. Ahmed, A. Khan, S. R. Chowdhury, R. Boutaba, and J. Mitra, "ReNoVatE: Recovery from node failure in virtual network embedding," in *Proc. 12th Int. Conf. Netw. Service Manage. (CNSM)*, Oct. 2016, pp. 19–27.
[19] F. Tonini, E. Amato, and C. Raffaelli, "Optimization of optical aggregation network for 5G URLLC service," in *Proc. IEEE Global Commun. Conf. (GLOBECOM)*, Dec. 2019, pp. 1–6.
[20] P. José S. Júnior, L. R. Costa, and A. C. Drummond, "On the efficiency and quality of protection of preprovisioning in elastic optical networks," 2022, *arXiv:2202.02415*.
[21] S. Ramamurthy, L. Sahasrabuddhe, and B. Mukherjee, "Survivable WDM mesh networks," *J. Lightw. Technol.*, vol. 21, no. 4, p. 870, Apr. 2003.
[22] D. T. Hai, "On routing, spectrum and network coding assignment problem for transparent flex-grid optical networks with dedicated protection," *Comput. Commun.*, vol. 147, pp. 198–208, Nov. 2019.

[23] A. E. Kamal, A. Ramamoorthy, L. Long, and S. Li, "Overlay protection against link failures using network coding," *IEEE/ACM Trans. Netw.*, vol. 19, no. 4, pp. 1071–1084, Aug. 2011.
[24] X. Shao, Y.-K. Yeo, Z. Xu, X. Cheng, and L. Zhou, "Shared-path protection in OFDM-based optical networks with elastic bandwidth allocation," in *Proc. OFC/NFOEC*, Mar. 2012, pp. 1–3.
[25] B. Chen, J. Zhang, Y. Zhao, C. Lv, W. Zhang, Y. Gu, S. Huang, and W. Gu, "A novel recovery algorithm for multi-link failures in spectrum-elastic optical path networks," in *Proc. Asia Commun. Photon. Conf. Exhib. (ACP)*, Nov. 2011, pp. 1–6.
[26] L. Guo, X. Wang, J. Cao, and X. Zheng, "Recovery escalation with load balancing and backup resources sharing in survivable WDM optical networks," *Photonic Netw. Commun.*, vol. 18, no. 3, pp. 393–399, Dec. 2009.
[27] W. Zheng, S. Liu, and X. Qi, "Multi-links recovery algorithm in survivable WDM optical network," *Photonic Netw. Commun.*, vol. 21, no. 1, pp. 39–44, Feb. 2011.
[28] F. He and E. Oki, "Shared protection-based virtual network embedding over elastic optical networks," *IEEE Trans. Netw. Service Manage.*, vol. 19, no. 3, pp. 2869–2884, Sep. 2022.
[29] H. D. Chantre and N. L. S. da Fonseca, "The location problem for the provisioning of protected slices in NFV-based MEC infrastructure," *IEEE J. Sel. Areas Commun.*, vol. 38, no. 7, pp. 1505–1514, Jul. 2020.
[30] C. Raffaelli, E. Amato, P. Monti, and F. Tonini, "Reliable slicing in optical metro networks with reconfigurable backup resources," in *Proc. 13th Int. Symp. Commun. Syst., Netw. Digit. Signal Process. (CSNDSP)*, Jul. 2022, pp. 863–866.
[31] E. Amato, F. Tonini, and C. Raffaelli, "Differentiated protection in 5G vehicular networks," in *Proc. AEIT Int. Conf. Electr. Electron. Technol. Automot. (AEIT AUTOMOTIVE)*, Nov. 2020, pp. 1–6.
[32] D. T. Hai, "Photonic network coding and partial protection in optical-processing-enabled network: Two for a tango," *Opt. Quantum Electron.*, vol. 54, no. 5, p. 282, May 2022.
[33] D. T. Hai, H. T. Minh, and L. H. Chau, "QoS-aware protection in elastic optical networks with distance-adaptive and reconfigurable modulation formats," *Opt. Fiber Technol.*, vol. 61, Jan. 2021, Art. no. 102364.
[34] R. Goscien, K. Walkowiak, and M. Klinkowski, "On the complexity of routing and spectrum allocation in survivable elastic optical network with unicast and anycast traffic," in *Proc. 8th Int. Workshop Resilient Netw. Design Modeling (RNDM)*, Sep. 2016, pp. 166–173.
[35] K. Christodoulopoulos, I. Tomkos, and E. A. Varvarigos, "Elastic bandwidth allocation in flexible OFDM-based optical networks," *J. Lightw. Technol.*, vol. 29, no. 9, pp. 1354–1366, May 2011.
[36] M. Moharrami, A. Fallahpour, H. Beyranvand, and J. A. Salehi, "Resource allocation and multicast routing in elastic optical networks," *IEEE Trans. Commun.*, vol. 65, no. 5, pp. 2101–2113, May 2017.
[37] E. E. Moghaddam, H. Beyranvand, and J. A. Salehi, "Routing, spectrum and modulation level assignment, and scheduling in survivable elastic optical networks supporting multi-class traffic," *J. Lightw. Technol.*, vol. 36, no. 23, pp. 5451–5461, Dec. 1, 2018.
[38] M. Aibin and K. Walkowiak, "Adaptive survivability algorithm for path protection with various traffic classes in elastic optical networks," in *Proc. 7th Int. Workshop Reliable Netw. Design Modeling (RNDM)*, Oct. 2015, pp. 56–62.
[39] K. D. R. Assis, R. C. Almeida, and H. Waldman, "Revenue optimization and protection with network slicing over a physical optical substrate," in *Proc. IEEE 22nd Int. Conf. High Perform. Switching Routing (HPSR)*, Jun. 2021, pp. 1–6.
[40] X. Wang, L. Wang, S. E. Elayoubi, A. Conte, B. Mukherjee, and C. Cavdar, "Centralize or distribute? A techno-economic study to design a low-cost cloud radio access network," in *Proc. IEEE Int. Conf. Commun. (ICC)*, May 2017, pp. 1–7.

NOURHAN REZK received the B.Sc. degree in electronics and communications from the Faculty of Engineering, Arab Academy for Science, Technology and Maritime Transport (AASTMT), Cairo, Egypt, in 2016, where she is currently pursuing the M.Sc. degree in electronics and communication engineering.

MOHAMED SHEHATA (Member, IEEE) received the Ph.D. degree in information engineering from the Department of Electronics, Information and Bioengineering (DEIB), Politecnico di Milano (Polimi), Italy, in 2019. He is currently an Assistant Professor with the Faculty of Engineering, Arab Academy for Science, Technology and Maritime Transport, Cairo, Egypt. His research interests include 5G radio access networks, cloud networks, applications of machine learning to wireless networks, energy efficiency, and network resiliency.

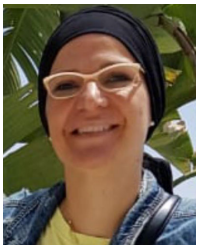

SAFA M. GASSER (Member, IEEE) received the Ph.D. degree in adaptive signal processing and control from the University of California at Santa Cruz, Santa Cruz. She has delivered the valedictory address at her graduation ceremony. She is currently an Associate Professor of communications with the Department of Electronics and Communications, Arab Academy for Science, Technology and Maritime Transport (AASTMT). Her research interests include adaptive signal processing, in addition to machine learning and remote sensing. She is a former Councilor of the IEEE AASTMT Chapter.

MOHAMED S. EL-MAHALLAWY received the B.Sc. and M.Sc. degrees from the Electronics and Communications Department, Faculty of Engineering, Arab Academy for Science, Technology and Maritime Transport, Egypt, in 1998 and 2002, respectively, and the Ph.D. degree in image processing and pattern recognition from Cairo University, Egypt, in 2008. He was a Postdoctoral Fellow with Universiti Technolgi Malaysia, from 2011 to 2012. He is currently a Professor with the Electronics and Communications Department, Faculty of Engineering, Arab Academy for Science, Technology and Maritime Transport.